Electron and Nuclear Positions in the Short Hydrogen Bond in Urotropine-*N*-oxide·Formic Acid

Cara L. Nygren,[†] Chick C. Wilson,[‡] and John F. C. Turner*[,†,||]

Department of Chemistry and Neutron Sciences Consortium, University of Tennessee, Knoxville, Tennessee 37996-1600, and Department of Chemistry, University of Glasgow, Glasgow, G12 8QQ, U.K.

Received: June 28, 2004; In Final Form: November 9, 2004

The crystal structure of urotropine-*N*-oxide·formic acid, as determined from multiple temperature single-crystal X-ray diffraction experiments in the range 123−295 K and from neutron diffraction at 123 K, is reported. There is a strong hydrogen bonding interaction between the OH of formic acid and the *N*-oxide of urotropine, with the oxygen−oxygen distance ranging from 2.4300(10) to 2.4469(10) Å. The electron density of the hydrogen atom associated with this interaction was located in the Fourier difference maps of the spherical atom refinement after all heavy atom positions were determined. The maximum of the electron density associated with the hydrogen bond is located approximately 1.16 Å from the formate segment, though the distribution of electron density is very broad. The electron density associated with the H atom is thus shown by these accurate X-ray diffraction experiments to be approximately centered at all temperatures studied. This was conclusively confirmed by single-crystal neutron diffraction data obtained at 123 K, from which statistically equivalent O−H distances of 1.221(7) and 1.211(7) Å were obtained.

1. Introduction

Hydrogen bonding is a common interaction in many areas of structural chemistry.[1−4] In chemically simple systems, such as the hydrides of the first-row elements, it is responsible for the strongly associated nature of water,[5−11] ammonia,[12] and hydrogen fluoride,[13−15] as well as the excellent solvent properties of these fluids. The physical and chemical properties of more complex systems are also due to the presence of the hydrogen bond; highly complex examples occur in structural biology, where the generation and maintenance of protein secondary and tertiary structure is dependent on this interaction.[2−4,8] Protein−protein interactions,[4] enzymatic catalysis,[2,3] and the structural chemistry of DNA are yet more complex examples.

The presence of a hydrogen bond is relatively simple to predict in the solid state. The presence of two electronegative atoms, usually N, O, or F, one of which is bound to at least one hydrogen, normally ensures that a hydrogen bond will exist, assuming that there is no structural motif that prevents bond formation. The ease of formation and the predictability of the presence of hydrogen bonds have led to the exploitation of this interaction in the intelligent design of crystal structures—the field of crystal engineering.[16−21]

Apart from the importance and flexibility of the hydrogen bond as an important interaction in the solid state, it is also of theoretical interest in the study of proton transfer in several systems: notably, carboxylic acid dimers have been investigated theoretically and experimentally toward this end.[22−31] It has been demonstrated, through both variable temperature X-ray and neutron diffraction experiments, that in some molecular systems the hydrogen atom migrates to the center of the X−H−Y bond as the temperature of the experiment is raised.[28,29,32,33] It is notable that proton migration may occur in both homonuclear (X−H−X) and heteronuclear (X−H−Y) systems. In this area, one of us (C.C.W.) has played a role in the application of neutron and X-ray diffraction at variable temperature to this type of problem; neutron diffraction has generally played an important role in the determination of nuclear positions for low-*Z* atom problems. A combination of neutron and X-ray diffraction permits a complete characterization of all scattering density present—the nuclear and electron densities associated with the H atom.

For many chemical systems, the determination of structure is based on the assumptions of the existence of atoms within the molecules; in this sense, a molecule may be defined as a bound ensemble of atoms and is therefore an extra hierarchical layer over and above the structure of the atom in the description of matter. Though this assumption is widespread in chemistry, a comprehensive definition of the atom within this hierarchical structure that is quantum mechanically satisfactory has only been derived in the past 25 years or so, predominantly due to the work of Bader.[34−39] More succinctly,[40] *[t]he molecular structure hypothesis—that a molecule is a collection of atoms linked by a network of bonds—was forged in the crucible of nineteenth century experimental chemistry. It has continued to serve as the principal means of ordering and classifying the observations of chemistry.*

An issue arises when considering the structure of a crystalline material that derives from the bipartile nature of the atom itself: it is not possible, by a single experimental method, to determine the structure of an atom or any ensemble of atoms; one may determine the electron density *or* the nuclear density, but not both, using the same radiation source. If the nuclear position of the atom and the electron density associated with the atom are very strongly correlated, then it is certainly reasonable to assert that either the distribution of the nuclear positions or the distribution of total electron density is a good

[†] Department of Chemistry, University of Tennessee.
[‡] University of Glasgow.
[||] Neutron Sciences Consortium, University of Tennessee.

10.1021/jp047187r CCC: $30.25
Published on Web 02/10/2005

measure of the position of any atom within the system. We also note that, for the vast majority of atoms, the total electron density is dominated by the core electron density.

There are at least two areas where this last generality is not true in molecular systems: the electrides[41−43] and those systems that contain the hydrogen bond. In the latter case, the valence density of hydrogen is also the "core" density and in the hydrogen bond the delocalized nature of the electron density ensures that the normally strong correlation between the distribution of nuclear density and the distribution of electron density breaks down. Consequentially, the "atomic" definition of a hydrogen bond is more problematic.

In this report, we detail extensive X-ray diffraction studies at variable temperature, as well as a neutron diffraction study, of urotropine-*N*-oxide·formic acid. By using both radiation sources, we thereby define all the scattering density in the Bragg average associated with the hydrogen bond. We note that the neutron diffraction data are not essential or even necessary in an a priori sense to define the electron density distribution in the hydrogen bond, but as we shall show, the inclusion of information about the distribution of nuclear density is instructive. Moreover, we explore the possible methods of visualization of the electron density associated with the hydrogen bond and show that direct, Fourier imaging is a useful method that is complementary to other, more usual methods of refinement.[44] We also explore the chemical ramification of our results in an "atomistic", chemical sense and show that such a description of the hydrogen bond is not particularly illuminating.

Urotropine is a molecular system that has had an important role in crystallography, due in part to the similarity of this molecule to adamantane.[45−58] Whereas adamantane is of great interest as an archetype for plasticity, urotropine is brittle,[59] despite the apparent similarity between the molecular structures. Urotropine crystallizes in the cubic space group $I4_3/m$, with one nitrogen atom and one carbon atom in the asymmetric unit, and is structurally related to adamantane. Due to the high tetrahedral symmetry of the molecule, there is only one set of unique bond lengths for urotropine and the C−N bond length is 1.4715(14) Å. The simplicity of the asymmetric unit and the lattice has ensured that urotropine has been investigated as a model for lattice dynamics,[53] molecular vibrations in the solid state,[47,49,50,52,53,56,60] and multipole refinements,[53,57,58] among other areas. Urotropine-*N*-oxide is a potentially polybasic, polar molecule, and its adducts are interesting systems for the investigation of hydrogen bonding. The molecule has two potential sites at which hydrogen bonding may occur—the tertiary nitrogen centers and the *N*-oxide O atom—offering the potential for the "engineering" of intermolecular interactions with appropriate adducts.

The molecular structure of urotropine-*N*-oxide, shown in Figure 1, has previously been investigated by single-crystal X-ray diffraction.[61] It is notable that the N−O bond length is particularly short at 1.3951(12) Å, where the normal range for the N−O distance in hydroxylammonium cations is 1.396−1.436 Å.[62,63] It is a neutral molecule, though there is a formal charge separation between nitrogen and oxygen. The structure of several adducts of urotropine-*N*-oxide have also been reported;[64−68] we note that the molecular and crystal structure of **1** was first determined by Mak in 1978, from data accumulated at room temperature.[67,68]

There is a potential coupling between the distribution of electron density associated with the hydrogen position and the structure of the formic acid residue in urotropine-*N*-oxide·formic acid, and in a valence bond, atomistic description, this correlation automatically is present. This possibility was alluded to by Mak in 1978 in an inverted manner by asserting that, due to the asymmetry in the C−O and C═O bond lengths, there was no formal proton transfer, though the quality of his data collected at that time precluded a detailed analysis of the structural behavior of the hydrogen atom. Correlation of the bond lengths in the formic acid residue to the structure of the electron density, and therefore the proton position, can occur in this material as full H atom transfer to the N−O bond should result in the formation of a delocalized formate ion. Retention of $O_{formate}$−H bond order should make the delocalization less likely in the formate ion. Possible equilibria of this type are shown in Figure 2.

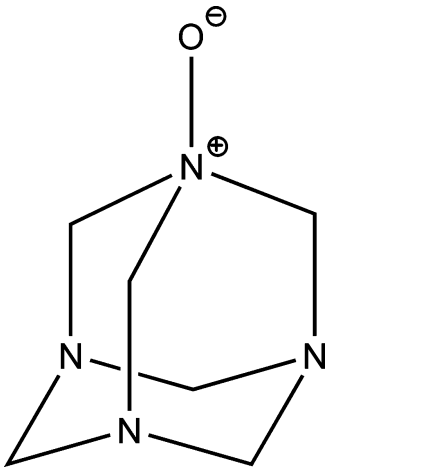

Figure 1. Molecular structure of urotropine-*N*-oxide.

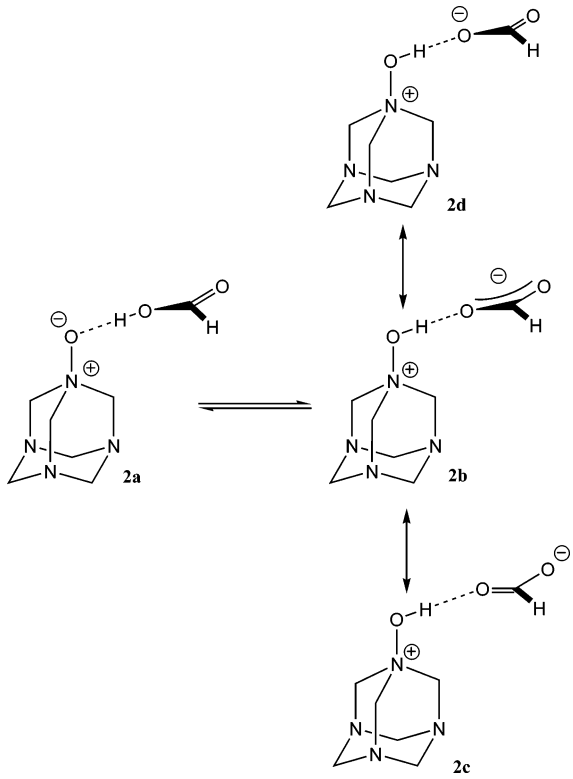

Figure 2. Potential equilibria involving both proton and electron redistribution.

Using a valence bond formalism, in principle, the *N*-oxide·formic acid adduct **2a** can equilibrate with **2b**, the hydroxylammonium formate salt where the formate ion is fully delocalized and therefore possesses equal C−O bond lengths, or

TABLE 1: Selected Refinement Parameters for the Collected Data

temp (K)	123 (neutron)	123 (X-ray)	148	173	198	223	248	298
θ range (deg)		2.10−28.34	2.10−28.34	2.11−28.31	3.10−28.27	2.10−28.34	2.10−28.29	2.10−28.79
index range for data collection	$-13 \le h \le 13$ $-13 \le k \le 2$ $-31 \le l \le 38$	$-9 \le h \le 8$ $-8 \le k \le 9$ $-25 \le l \le 25$	$-9 \le h \le 8$ $-8 \le k \le 9$ $-25 \le l \le 25$	$-9 \le h \le 8$ $-8 \le k \le 8$ $-24 \le l \le 25$	$-9 \le h \le 8$ $-9 \le k \le 8$ $-25 \le l \le 25$	$-8 \le h \le 8$ $-9 \le k \le 9$ $-25 \le l \le 25$	$-8 \le h \le 8$ $-9 \le k \le 9$ $-25 \le l \le 25$	$-9 \le h \le 9$ $-9 \le k \le 9$ $-25 \le l \le 25$
reflns collected	3771	9144	9144	9107	8748	9329	9177	9415
independent reflns [R(int)]	2144	2145 [0.0232]	2145 [0.0232]	2143 [0.0226]	2144 [0.0216]	2176 [0.0279]	2168 [0.0216]	2195 [0.0252]
completeness to $\theta = 28.33°$ (%)		97.1	97.1	97.1	96.6	97.3	97.1	92.8
data/restraints/params	2144/0/313	2145/0/131	2145/0/131	2143/0/131	2144/0/131	2176/0/131	2168/0/131	2195/0/131
S	1.02	1.037	1.037	1.045	1.043	1.014	1.025	1.017
final R indices	R1 = 0.151[a] $wR^2 = 0.092$[a]	R1 = 0.0349[a] $wR^2 = 0.0990$[a]	R1 = 0.0349[a] $wR^2 = 0.0990$[a]	R1 = 0.0359[a] $wR^2 = 0.0973$[a]	R1 = 0.0355[b] $wR^2 = 0.0992$[b]	R1 = 0.0379[b] $wR^2 = 0.1012$[b]	R1 = 0.0398[b] wR^2 =0.1039[b]	R1 = 0.0409[b] $wR^2 = 0.1056$[b]
R indices (all data)	R1 = 0.221 $wR^2 = 0.095$	R1 = 0.0393 $wR^2 = 0.1043$	R1 = 0.0393 $wR^2 = 0.1043$	R1 = 0.0414 $wR^2 = 0.1025$	R1 = 0.0386 $wR^2 = 0.1030$	R1 = 0.0490 $wR^2 = 0.1120$	R1 = 0.0501 $wR^2 = 0.1126$	R1 = 0.0555 $wR^2 = 0.1153$

[a] $[I > 2\sigma(I)]^X$, $[I > 3\sigma(I)]^N$. [b] $[I > 2\sigma(I)]$.

with **2c**/**2d**, the hydroxylammonium formate salts where the bond lengths in the formate ion are not resonance delocalized.

We note that the resonance structures illustrated in Figure 2 as intermediates only have formal meaning within a valence bond description and that the description of many main group and organic molecules is inadequate when the description is based on a hybridizational or valence bond approach.[69−76] By using a method of analysis which expressly uses a delocalized description of the electron density, we hope to shed light on the precise nature of the hydrogen bonding network in **1**.

2. Experimental Section

Urotropine-*N*-oxide·formic acid was synthesized by addition of an excess of hydrogen peroxide to an aqueous solution of urotropine. Single crystals suitable for X-ray or neutron diffraction experiments were either grown by slow evaporation of the reaction mixture or recrystallized from concentrated aqueous solutions by passing a current of air over a droplet of the solution that was placed on a glass plate made hydrophobic by the application of a very small quantity of sebaceous oil.

X-ray Diffraction Experiments. For the temperature range 123−198 K, suitable crystalline specimens were mounted in Paratone oil, while for temperatures of 223 K to room temperature the crystals were mounted with epoxy on a glass fiber. Single-crystal X-ray diffraction data were collected using a Bruker AXS Smart 1000 Diffractometer equipped with a CCD area detector and graphite monochromatized Mo source (Mo Kα, 0.710 73 Å) and a Nicolet LT-2 cooling device, with a crystal-to-detector distance of 5.0 cm. Diffraction data were collected from crystalline specimens of urotropine-*N*-oxide·formic acid at temperatures of 123, 148, 173, 198, 223, 248, and 298 K; the parameters of each data collection are collated in Table 1.

Refinement of X-ray Data. More than a hemisphere of data were collected over the angular range of 2.10−28.34° in θ (123 K).[77] Frame widths of 0.3° were used for the data collection of 9144 reflections, counting 40 s per frame. Data reduction and spherical atom analyses were carried out using the Bruker program Saint[78] and the General Structure Analysis System (GSAS).[79] The unit cell dimensions were refined on the basis of 7531 reflections. A multiscan absorption correction was made using SADABS.[80] Systematic absences were consistent with the space group $P2_1/n$. A total of 8163 reflections were collected, and merging of equivalent reflections gave 2145 unique reflections ($R_{int} = 2.32\%$), with 2004 classed as observed ($|F_o| > 4\sigma_F$). The structure was solved by direct methods (SHELXTL),[44] refined by the full matrix least-squares method and completed by a series of difference Fourier syntheses. All non-hydrogen atoms were refined anisotropically, with most of the hydrogen atoms being introduced at idealized positions and refined using a riding model. The electron density associated with H1, the hydrogen bonded H atom, was located in the Fourier difference map and its positional parameters refined. Thermal parameter refinements for the hydrogen bonded H atom were performed using SHELXTL[44] for isotropic refinements and GSAS[79] for anisotropic refinements. Weighted R-factors, wR^2, and all goodness-of-fit values are based on F^2.

Neutron Diffraction Experiments. Neutron diffraction data were obtained at the Intense Pulsed Neutron Source (IPNS) at Argonne National Laboratory using the time-of-flight Laue single-crystal diffractometer (SCD).[81,82] At the IPNS, pulses of protons are accelerated into a heavy-element target 30 times per second to produce pulses of neutrons by the spallation process. Because of the pulsed nature of the source, neutron wavelengths are determined by time of flight based on the de Broglie equation

$$\lambda = \frac{hm}{tl}$$

where h is Planck's constant, m is the neutron mass, and t is the time of flight for a flight path l, so that the entire thermal spectrum of neutrons can be used. With position-sensitive area detectors and a range of neutron wavelengths, a solid volume of reciprocal space is sampled with each stationary orientation of the sample and the detectors. The SCD has two ^{6}Li-glass scintillation position-sensitive area detectors, each with active areas of 15 × 15 cm^2 and a spatial resolution of <1.5 mm. One of the detectors is centered at a scattering angle of 75° and a crystal-to-detector distance of 23 cm, and the second detector is at 120° and 18 cm. Details of the data collection and analysis procedures have been published previously.[81,82]

A crystal of urotropine-*N*-oxide·formic acid with approximate dimensions of 1.8 × 1.3 × 0.6 mm^3 was molded into an aluminum foil "sandwich" and was glued to the end of a standard aluminum pin with epoxy adhesive. The sample was placed on the DISPLEX cold stage in the SCD, cooled to 260 K in a helium atmosphere, and then cooled to 123 K under vacuum.

For each setting of the diffractometer angles, data were stored in three-dimensional histogram form with coordinates x,y,t corresponding to horizontal and vertical detector positions and the time of flight, respectively. Data were analyzed using the ISAW software package[83] in addition to other local IPNS SCD programs. For intensity data collection, runs of 6 h per histogram were initiated, arranged at χ and φ values suitable to cover at

TABLE 2: Lattice Parameters (Reduced Unit Cell) for the Collected Data at Variable Temperature[a]

a/Å	*b*/Å	*c*/Å	β/deg	*T*/K	ref
6.845	6.847	19.480	95.06	298	67
6.726(1)	6.732(1)	19.418(4)	95.391(16)	123	this work$^{(N)}$
6.774(2)	6.790(2)	19.472(7)	95.159(6)	123	this work$^{(X)}$
6.7679(19)	6.779(2)	19.487(6)	95.446(5)	148	this work$^{(X)}$
6.770(3)	6.799(3)	19.433(8)	95.297(7)	173	this work$^{(X)}$
6.787(2)	6.802(2)	19.532(7)	95.266(6)	198	this work$^{(X)}$
6.785(2)	6.8176(19)	19.473(6)	95.107(1)	223	this work$^{(X)}$
6.7989(5)	6.8226(4)	19.4639(13)	95.1020(10)	248	this work$^{(X)}$
6.8272(13)	6.8456(13)	19.484(4)	94.983(3)	298	this work$^{(X)}$

[a] The superscripts in the reference column denote X-ray (X) versus neutron (N) data.

TABLE 3: Intermolecular Structural Parameters at Variable Temperature from Spherical Atom Refinement[a]

T/K	r_{N1O1}/Å	r_{O1H1}/Å	r_{O2H1}/Å	r_{O1O2}/Å	r_{O2C7}/Å	r_{O3C7}/Å	$\angle_{O1H1O2}$/deg	$\angle_{O2C7O3}$/deg	
123	1.3727(33)	1.221(7)	1.211(7)	2.428(6)	1.286(5)	1.230(4)	173.3(6)	126.28(34)	(N)
123	1.3984(11)	1.24(4)	1.19(7)	2.435(1)	1.2862(14)	1.2228(13)	173.1(5)	125.17(10)	(X)
148	1.3956(11)	1.25(3)	1.21(3)	2.443(1)	1.2818(15)	1.2252(15)	170.0(6)	125.62(11)	(X)
173	1.3949(12)	1.24(2)	1.21(2)	2.439(1)	1.2778(15)	1.2206(15)	172.3(6)	125.55(12)	(X)
198	1.3951(11)	1.24(6)	1.20(6)	2.438(1)	1.2786(15)	1.2234(15)	174.0(6)	125.89(12)	(X)
223	1.3979(12)	1.22(6)	1.24(6)	2.450(1)	1.2757(16)	1.2258(15)	174.2 (6)	126.05(12)	(X)
248	1.3933(13)	1.26(3)	1.18(6)	2.430(1)	1.2680(18)	1.2147(18)	172.7(6)	126.00(15)	(X)
298	1.3940(14)	1.27(6)	1.18(3)	2.430(1)	1.263(2)	1.2107(19)	171.4(1)	126.47(16)	(X)
298	1.388(6)			2.435(4)	1.281(6)	1.200(6)		126.1(5)	67

[a] Neutron data are represented by "(N)" and X-ray data by "(X)".

least one unique quadrant of reciprocal space. With this counting time, 17 histograms were completed during the 5 days available for the experiment. The recorded histograms were indexed and integrated using individual orientation matrices for each histogram, to allow for any misalignment of the sample. The intensities were corrected for wavelength dependence of the incident spectrum and sample absorption (μ (cm^{-1}) = 4.205).

Refinement of Neutron Data. Bragg reflections were integrated about their predicted location and were corrected for the Lorentz factor, the incident spectrum, and the detector efficiency. A wavelength-dependent spherical absorption correction was applied using cross sections from Sears[84] for the non-hydrogen atoms and from Howard et al.[85] for the hydrogen atoms. Symmetry-related reflections were not averaged since different extinction factors are applicable to reflections measured at different wavelengths. The GSAS software package was used for structural analysis.[79] The atomic positions of the X-ray diffraction structure were used as a starting point in the refinement. All atoms including hydrogen atoms were refined with anisotropic thermal parameters. The refinement used 313 variables and converged to $R_w(F^2) = 0.092$ and $R(F^2) = 0.151$. Data collection and refinement parameters are summarized in Table 1. A compilation of the lattice parameters for both the neutron data and the variable temperature X-ray data are found in Table 2.

3. Results

Molecular and Crystal Structure. The symmetry of free urotropine-*N*-oxide is C_{3v}, and therefore the carbon−nitrogen bond lengths are no longer equivalent. The carbon−nitrogen bond lengths adjacent to the *N*-oxide portion are considerably lengthened compared to the carbon−nitrogen bond distances which are further removed from the charge-separated segment of the molecule.[62,63,67] The three nitrogen−carbon bond distances (for the nitrogen atom of the *N*-oxide portion) are elongated to an average distance of 1.5411(18) and 1.5249(13) Å for the room temperature and 123 K X-ray diffraction study, respectively. The remaining nitrogen−carbon bond distances are similar to those of free urotropine-*N*-oxide [1.441(2) and 1.473(2) Å, 298 K; 1.4480(14) and 1.4783(14) Å, 123 K].[61,68] Based on the neutron diffraction data, the carbon−oxygen bond distances in the formate segment of the molecule are 1.286(5) and 1.230(4) Å for the C7−O2 and C7−O3 bonds, respectively, and these distances are compiled in Table 3. These distances coincide with the results extracted from the X-ray diffraction experiment at 123 K, 1.2862(14) and 1.2228(13) Å, respectively. The C−N bond distances in the cage correspond well with the distances obtained in the X-ray diffraction experiment, differing by less than 0.001 Å.

The gross molecular structure, determined by spherical atom refinements of the X-ray data, is unsurprising and the non-hydrogenous structure remains relatively invariant with temperature. Relevant structural parameters are given in Table 3. A representative structure of the asymmetric unit is shown in Figure 3a, with the corresponding packing diagram in Figure 3b. The latter shows the orientation of the four molecules that are contained in the unit cell. It is notable that the packing segregates the more polar parts and less polar parts of the complex; the polar portions, consisting of the *N*-oxide and the hydrogen bound formic acid, are mutually anti to each other across the sheet composed of less polar cages.

Hydrogen Bond Structure. Urotropine-*N*-oxide has four potential sites at which hydrogen bonding may occur: there is one electronegative oxygen atom and three tertiary amines which may act as potential strong hydrogen bond acceptors. Examination of extended contacts in the unit cell using Mercury[62,86] revealed that the only substantial interaction was the short, strong hydrogen bond present between the urotropine-*N*-oxide and the formate residue. The observed hydrogen bond in this case is to the *N*-oxide O atom, with a short oxygen−oxygen distance ranging from 2.4300(10) Å to 2.4469(10) Å based on the X-ray data and 2.428(7) Å in the neutron data at 123 K. This lies well within the standard definition for a short very strong hydrogen bond,[87] which is defined as one where the O···O lies in the range 2.2−2.5 Å.

In addition to the "very strong" hydrogen bond between the oxygen atom of the *N*-oxide, O1, and the oxygen atom, O2, of the formate segment, there are three other hydrogen bonds

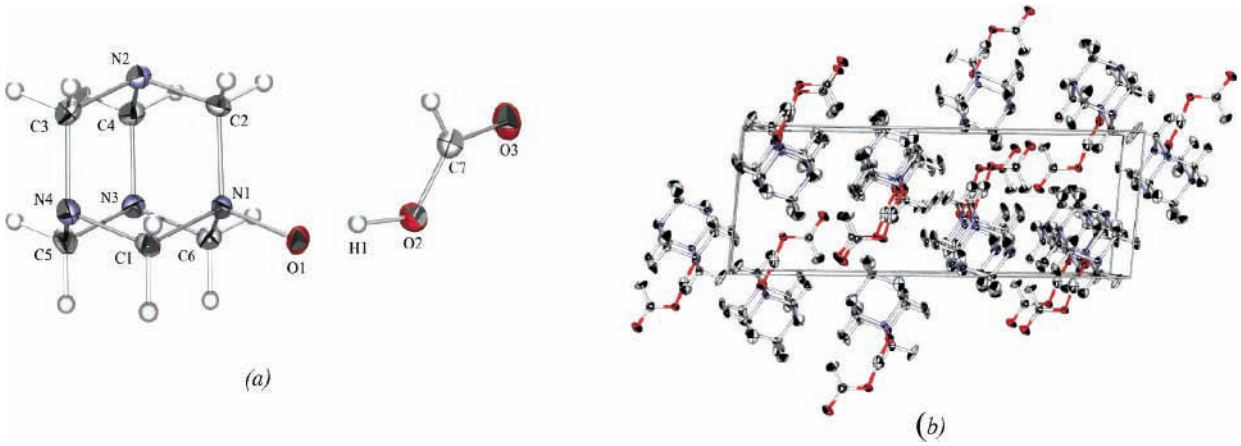

Figure 3. Molecular structure of urotropine-*N*-oxide·formic acid at 123 K (a) and packing diagram (b).[93]

present in this system. Each of the three tertiary amines forms a hydrogen bond to an adjacent molecule, which may be classified as a "weak" hydrogen bond,[87] with N···H bond distances ranging from 2.68 to 2.89 Å.[62,86] However, it is notable that the van der Waals sum for N···H is 2.75 Å,[88] and it may therefore be more appropriate to classify the N···H interaction as a hydrogen bridge.[16,87,89]

Nuclear Structure of the Hydrogen Bond. The results of the neutron diffraction experiment at 123 K reveal the nuclear position of the H atom associated with the hydrogen bond. The proton is located 1.221(7) Å from the oxygen atom of the *N*-oxide segment of the molecule and 1.211(7) Å from O2 of the formate segment, with an O1−H1−O2 angle of 173.3(6)°. Therefore, within the errors associated with the experiment, this results in a short symmetric hydrogen bond.

Discussion

It has recently been shown that direct imaging of hydrogen density from X-ray diffraction experiments can be more reliable than parameters determined from refinements;[33,90] this is particularly true in the case of elongated or highly anisotropic density as observed in this system. However, our multiple temperature study, and the apparent invariance of the shape and position of the difference Fourier peak representing the electron density associated with H1, allows us to conclude that in this system the hydrogen atom is strongly perturbed toward a position close to the center of the O···O vector and its position appears invariant (within the accuracy of the X-ray data) as a function of temperature. This is a significant observation, particularly in light of several recent reports of migration of the H atom in such cases;[28,29,32,33] the nature of the hydrogen bond in urotropine-*N*-oxide·formic acid is robust toward such effects.

The distribution of electron density in the Fourier difference maps in Figure 4 (calculated in the absence of H1 from the model) in the region of the short, strong hydrogen bond shows elongation of the density along the O1−O2 vector, commonly observed in short, strong hydrogen bonds. As seen in the Fourier maps, the maximum in the electron density associated with the hydrogen bond is located approximately 1.16 Å from the formate segment of the molecule, representing a significant elongation of the O−H "covalent" bond, where the electron density is distributed between O and H over a length of ∼1 Å, and is indicative of a centered proton which is frequently observed in short hydrogen bonded systems. However, this distribution is broad and full quantification of the O−H distances in this system is complicated by the uncertainty introduced by the nature of the density representing this hydrogen atom.

Analysis of the neutron diffraction data at 123 K revealed the position of the proton associated with the hydrogen atom in the hydrogen bond: the distances between the proton position and the two oxygen atoms are $r_{H1O1} = 1.221(7)$ Å and $r_{H_1O_2} = 1.211(7)$ Å, with a bond angle $\angle_{O_1\hat{H}_1O_2} = 173.3(6)°$.

The relative invariance of the hydrogen atom position with temperature is also borne out by the trends in the other bond lengths in the system. For example, there is also a considerable change in the bond distances of the formic acid segment, which tend to increase as the temperature is lowered (possibly partly due to thermal parameter effects) and do not show a pattern consistent with transfer of the proton across the hydrogen bond. At room temperature, the carbon−oxygen double bond is 1.2107(19) Å and the C−O single bond is 1.263(2) Å. These bond distances are in accord with earlier studies of urotropine-*N*-oxide·formic acid as well as with studies of free formic acid as seen in a search of the Cambridge Structural Database (CSD).[62,63] As the temperature of the diffraction experiment was lowered to 148 K, the carbon−oxygen bond distances in the formic acid segment of the structure were both found to lengthen. The carbon−oxygen that is formally considered a single bond is 1.2818(15) Å, while the double bond is 1.2252-(15) Å, and a comparison of the bond lengths in the formate segment of the molecule are shown in Figure 5. These distances are closely related to a formic acid fragment which is hydrogen bound to another species.[62,63]

At 123 K, the heavy atom positions and the bond lengths derived from the data show a strong correlation between the X-ray and neutron data. However, there is not a strong correlation for the H atom. Given the experimental data, it may be assumed that the correlation of the heavy atom holds true at all temperatures. The carbon−oxygen bonds in the formate segment do not show any evidence of structures **2b** or **2c** shown in Figure 2. We note that, in the presence of a short, strong hydrogen bond, a similar lack of correlation in the carbon−oxygen bond lengths has been observed in other compounds where H atom transfer is observed.[91] There is no distinct difference in the two carbon−oxygen distances, which is to be expected from a valence bond description of the molecule. Also, the C−O bond lengths in the formate segment vary with temperature, which is unrelated to any structural change in the hydrogen bond. This indicates a resonance structure between **2a** and **2d** in Figure 2. Therefore, one cannot make assertions about the hydrogen bond based solely on heavy atom positions and bond lengths.

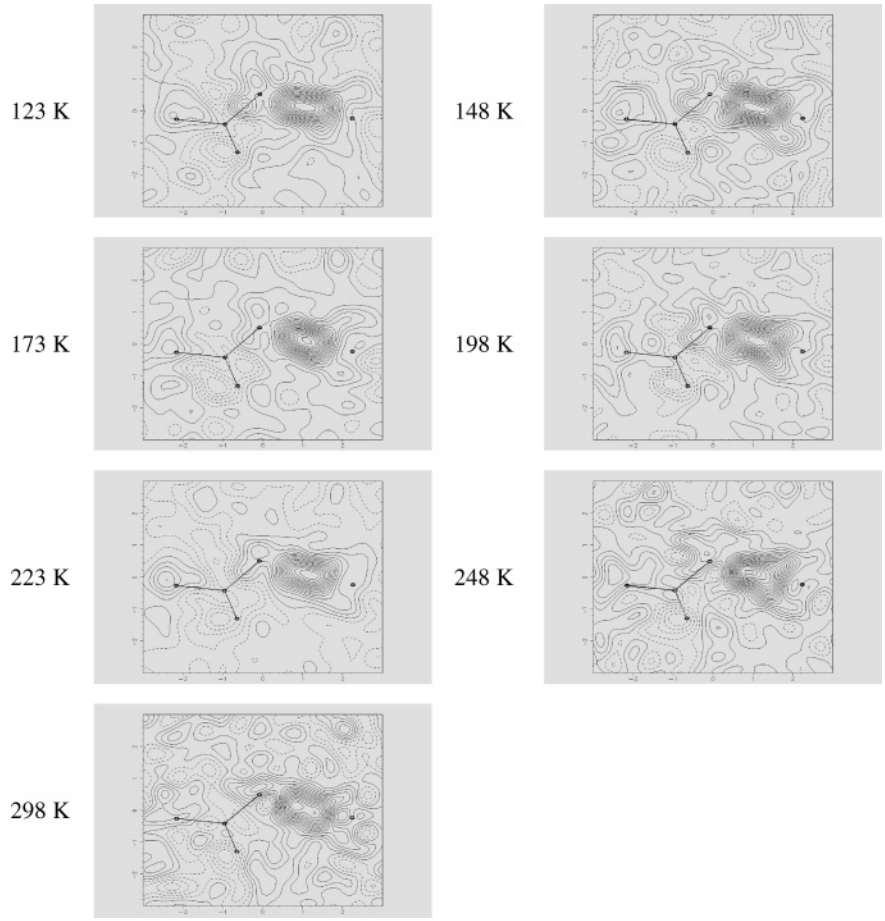

Figure 4. Fourier difference maps showing the electron density associated with the proton position of the formic acid OH.[94] Contour levels are drawn at 0.03 e Å^{-3}.

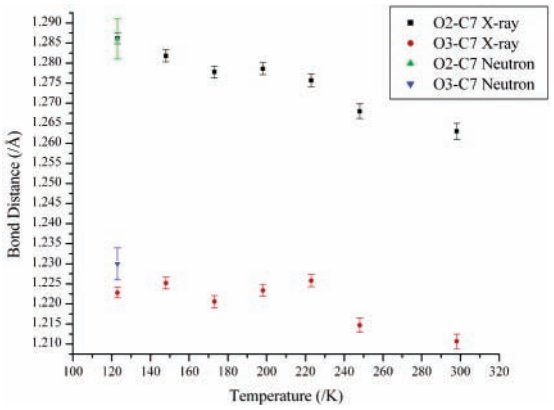

Figure 5. Comparison of the variation of C−O and C═O bond lengths of the formate segment by neutron diffraction and variable temperature X-ray diffraction experiments.

The partial "transfer" of the proton to the center of the short hydrogen bond, indicated by the difference Fourier maps, is supported by analysis of the N−O bond distance in the system. This is considerably longer than in free urotropine-*N*-oxide (1.363 Å) and slightly longer than previously known urotropine-*N*-oxide hydrogen bonded systems (1.380−1.391 Å) as seen in a search of the CSD.[62,63] The formation of a significant bonding interaction with the partly transferred proton withdraws electron density from the N−O bond, weakening the strength of the bond and therefore increasing the bond length. The average bond distance for the N−O bond in hydroxylammonium cations, as seen in a search of the Cambridge Structural Database, is 1.417-(2) Å, with a range from 1.396 to 1.436 Å.[62,63] This bond length corresponds more directly to urotropine-*N*-oxide·formic acid than does the average bond length for a typical *N*-oxide system. Once again the relative invariance of this N−O distance with temperature supports the stability of the "partly transferred" proton in this hydrogen bonding system.

For a comparative study of the bond lengths in the formic acid segment of the structure, single-crystal X-ray diffraction data were collected for rubidium hydrogen formate at 173 K using the data collection strategy as described above for urotropine-*N*-oxide·formic acid. There is a considerable amount of hydrogen bonding present in the solid-state structure of this material. The hydrogen bonds exist between two formic acid segments, with an oxygen−oxygen distance of 2.4360(13) Å. In the crystal structure, rubidium is 8-coordinate, with bond distances to the oxygen atoms of the formate ranging from 2.8853(13) to 3.1556(12) Å. The bond distances for the C−O single and double bonds were found to be 1.272(2) and 1.2269-(19) Å, respectively. These distances are similar to those found at the same temperature in urotropine-*N*-oxide·formic acid, 1.2778(15) and 1.2206(15) Å. Accordingly, the O−C−O angle in rubidium formate, 125.06(15)°, is only slightly smaller than that in urotropine-*N*-oxide·formic acid [125.55(12)°]. The lengthened bond distances demonstrate the strengthening of the hydrogen bond present between formic acid and urotropine-*N*-oxide as well as the migration of the electron density associated with the proton position as the temperature is lowered.

An anisotropic displacement parameter (ADP) may be defined as "the second moment of atomic probability distribution function".[92] This, in essence, describes the average displacement of atoms in crystals from the mean atomic positions in the Bragg

TABLE 4: Anisotropic Displacement Parameter Tensors for H1 from Neutron and X-ray Diffraction Data[79] [a]

U_{11}	U_{12}	U_{13}	U_{22}	U_{23}	U_{33}	U_{aniso}	
0.043(4)	0.0035(24)	0.0048(29)	0.0201(29)	0.0013(25)	0.028(4)	0.03032	H1 neutron
0.151(22)	0.031(13)	0.051(14)	0.038(11)	0.018(8)	0.047(13)	0.08263	H1 X-ray

[a] The average U_{aniso} for the H atoms in the urotropine cage is 0.03404 Å^2 (neutron data).

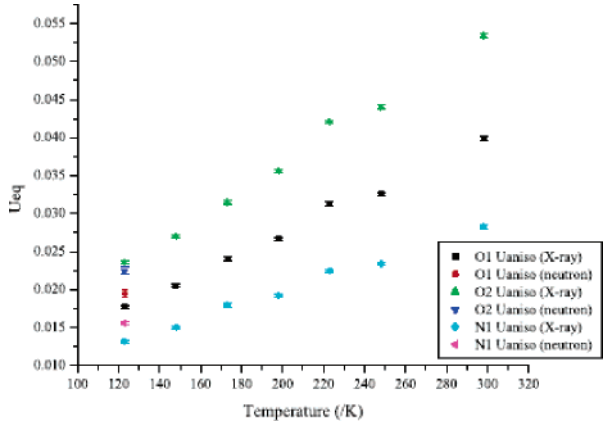

Figure 6. Comparison of U_{aniso} between neutron and X-ray data for the atoms most directly affected by the hydrogen bond (N1, O1, O2).

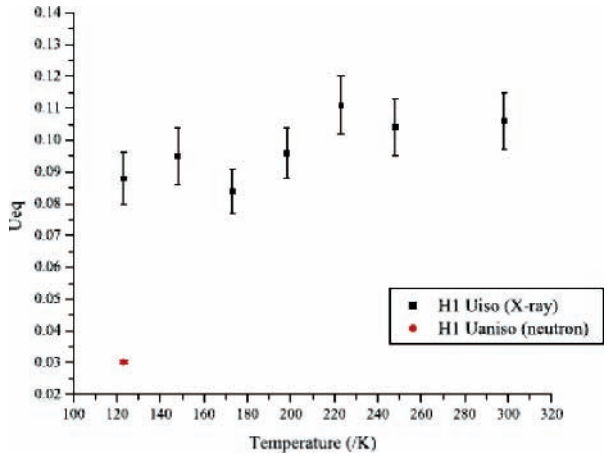

Figure 7. Comparison of results from neutron (U_{aniso}) and X-ray (U_{iso}) data for the hydrogen bonded H atom, H1.

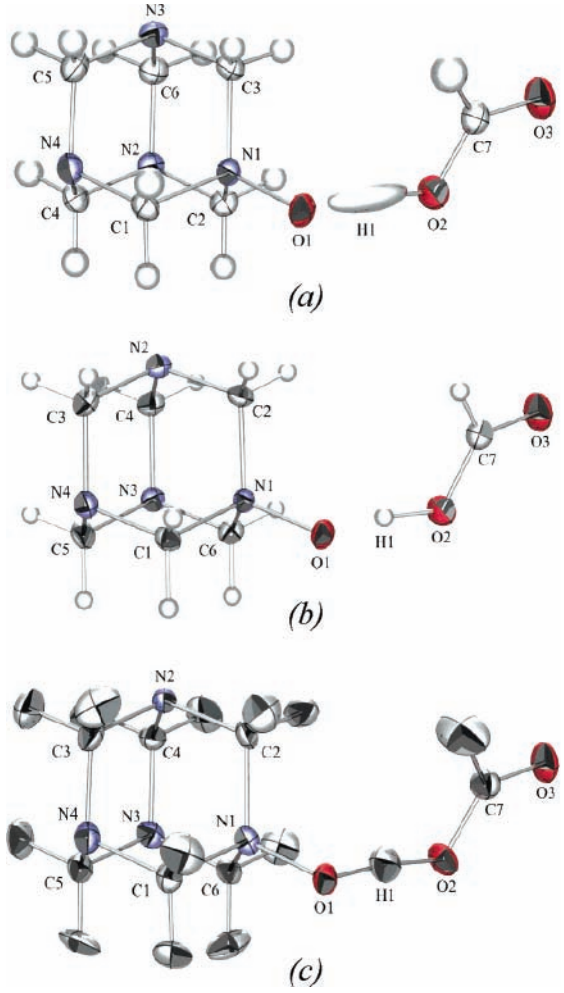

Figure 8. Comparison of X-ray and neutron data at 123 K: (a) X-ray data with anisotropic refinement of H1 using GSAS;[79] (b) X-ray data with isotropic refinement from SHELXTL;[44] (c) neutron data with anisotropic refinement of all H atoms from GSAS. Thermal ellipsoids are drawn at the 50% probablility level using POV-Ray.[93]

average. Figure 7 depicts the variation in U_{eq} with temperature for the X-ray data, as well as a comparison of the neutron data, for the atoms that are most affected by the presence of the hydrogen bond, namely N1, O1, and O2. In comparing the neutron and X-ray data at 123 K, it is notable that there is very little difference in U_{eq} for any of these atoms, the difference being approximately 0.001 Å^2. The major difference in the thermal parameters between the neutron and X-ray data is best shown in Figure 7, which represents H1, the hydrogen bonded H atom. Table 4 shows the anisotropic thermal parameter tensor components, U_{ij}^X and U_{ij}^N, of H1 extracted from the refinement of the X-ray and neutron data, respectively, and it shows the difference in ADPs (U_{iso} for X-ray data, U_{aniso} for neutron data) between the two sets of experiments. For a hydrogen atom, the valence electron density is also the core electron density, which leads to the diminished correlation between the distributions of nuclear and electron densities. From Figures 5 and 6 it is clear that the description of isotropic displacement parameters for the hydrogen atom from X-ray data is inadequate. Though results from the X-ray and neutron diffraction experiments showed very similar positional parameters for H1 in that the position of maximum electron density from the X-ray data corresponds well to the position of the proton in the neutron data, the ADPs clearly differ. In the refinement of neutron diffraction data, the ADPs of the proton position associated with the hydrogen bond are consistent with the average displacement over the thermally populated normal coordinates and lattice modes, and in this respect the ADPs of the proton are not anomalous when compared to the other atomic ADPs in the crystal. Therefore, given the broad distribution of electron density associated with the hydrogen bond, the use of ADPs to refine the structural parameters of the electron density associated with the hydrogen bond is clearly not in accord with the definition of the ADP. The neutron diffraction refinement of the O−H−O positions and ADPs effectively define the nuclear potential in which the four electrons associated with the hydrogen bond are confined. From inspection of the ADPs associated with the nuclear potential, it is clear that the motions of the atoms are smaller in magnitude than have been interpreted from the refined ADPs for the "H atom" associated with the hydrogen bond. It is therefore clear that parametrization of structural parameters of the distribution of electron density using ADPs is not physically

realistic within the structural definition of the ADP. Moreover, it is clear that a standard "spherical atom and ADP" model is inadequate to describe this distribution. However, we note that the Bragg scattering experiment is a priori an elastic experiment and contains no dynamic information about the system.

Given the physical ambiguity implied in using ADPs to define the structure of the distribution of electron density in a system in which there is a poor correlation between the nuclear and core electron density distributions, it is clear that direct imaging of electron density via a Fourier synthesis gives good qualitative information in this case. We note that more advanced aspherical methods are available which will allow a more precise quantitative description in these cases.

The results of spherical atom refinements using anisotropic atomic displacement parameters to model the distribution of electron density in the bond are shown in Figure 8a, together with an isotropic refinement of the electron density (Figure 8b) and the result of the neutron diffraction experiment (Figure 8c).

Conclusion

The proton in the short, strong hydrogen bond (O···O separation ∼2.44 Å) in the molecular complex urotropine-*N*-oxide·formic acid is partly transferred to the center of the hydrogen bond. The position of maximum density associated with the hydrogen atom in the hydrogen bond, indicated by difference Fourier syntheses, is found to be invariant with temperature in the range 123−298 K. This invariance is a significant indication of the stability of this hydrogen bond with respect to variations in temperature, in contrast to recent observations of proton migration in several similar hydrogen bonded systems. It is clear that trends in bond lengths between heavy atoms is not necessarily a good indicator of hydrogen atom behavior. The subtle interplay of intra- and intermolecular forces and lattice effects clearly mitigates in this case against motion of the proton along the bond.

Acknowledgment. J.F.C.T. acknowledges the financial support of the University of Tennessee, through provision of startup funds and through the establishment of the Neutron Sciences Consortium, and the Petroleum Research Fund, administered through the American Chemical Society (PRF-37341-G4). C.C.W. acknowledges this work was funded in part by EPSRC under Grant GR/R04690. The authors thank Arthur J. Shultz for discretionary beam time on SCD and experimental help. This work has benefited from the use of the Intense Pulsed Neutron Source at Argonne National Laboratory, which is funded by the U.S. Department of Energy, BES-Materials Science, under Contract W-31-109-Eng-38.

Supporting Information Available: Variable temperature X-ray diffraction data. This information is available free of charge via the Internet at http://pubs.acs.org.

References and Notes

(1) Steiner, T. *Angew. Chem., Int. Ed.* **2002**, *41*, 48−76.
(2) Schowen, K. B.; Limbach, H. H.; Denisov, G. S.; Schowen, R. L. *Biochim. Biophys. Acta* **2000**, *1458*, 43−62.
(3) Cleland, W. W. *Arch. Biochem. Biophys.* **2000**, *382*, 1−5.
(4) Perrin, C. L.; Nielson, J. B. *Annu. Rev. Phys. Chem.* **1997**, *48*, 511−544.
(5) Urquidi, J.; Benmore, C. J.; Egelstaff, P. A.; Guthrie, M.; McLain, S. E.; Tulk, C. A.; Klug, D. D.; Turner, J. F. C. *Mol. Phys.* **2004**, *102*, 2007−2014.
(6) George, W. O.; Jones, B. F.; Lewis, R. H. *Philos. Trans. R. Soc. London, Ser. A: Math., Phys. Eng. Sci.* **2001**, *359*, 1611−1629.
(7) Soper, A. K. *Chem. Phys.* **2000**, *258*, 121−137.
(8) Soper, A. K. *Physica B (Amsterdam)* **2000**, *276−278*, 12−16.
(9) Soper, A. K.; Ricci, M. A. *Phys. Rev. Lett.* **2000**, *84*, 2881−2884.
(10) Soper, A. K. *J. Phys.: Condens. Matter* **1996**, *8*, 9263−9267.
(11) Tromp, R. H.; Postorino, P.; Neilson, G. W.; Ricci, G. W.; Ricci, M. A.; Soper, A. K. *J. Chem. Phys.* **1994**, *101*, 6210−6215.
(12) Ricci, M. A.; Nardone, M.; Ricci, F. P.; Andreani, C.; Soper, A. K. *J. Chem. Phys.* **1995**, *102*, 7650−7655.
(13) McLain, S. E.; Benmore, C. J.; Siewenie, J. E.; Urquidi, J.; Turner, J. F. C. *Angew. Chem., Int. Ed.* **2004**, *43*, 1952−1955.
(14) Pfleiderer, T.; Waldner, I.; Bertagnolli, H.; Todheide, K.; Fischer, H. E. *J. Chem. Phys.* **2000**, *113*, 3690−3696.
(15) Deraman, M.; Dore, J. C.; Powles, J. G.; Holloway, J. H.; Chieux, P. *Mol. Phys.* **1985**, *55*, 1351−1367.
(16) Desiraju, G. R. *Acc. Chem. Res.* **2002**, *35*, 565−573.
(17) Desiraju, G. R. *Dalton* **2000**, 3745−3751.
(18) Holman, K. T.; Pivovar, A. M.; Swift, J. A.; Ward, M. D. *Acc. Chem. Res.* **2001**, *34*, 107−118.
(19) Nangia, A.; Desiraju, G. R. *Acta Crystallogr., Sect. A: Found. Crystallogr.* **1998**, *A54*, 934−944.
(20) Subramanian, S.; Zaworotko, M. J. *Coord. Chem. Rev.* **1994**, *137*, 357−401.
(21) Aakeroy, C. B.; Seddon, K. R. *Chem. Soc. Rev.* **1993**, *22*, 397−407.
(22) Wozniak, K.; Mallinson, P. R.; Smith, G. T.; Wilson, C. C.; Grech, E. *J. Phys. Org. Chem.* **2003**, *16*, 764−771.
(23) Wilson, C. C.; Goeta, A. E. *Angew. Chem., Int. Ed.* **2004**, *43*, 2095−2099.
(24) Mallinson, P. R.; Smith, G. T.; Wilson, C. C.; Grech, E.; Wozniak, K. *J. Am. Chem. Soc.* **2003**, *125*, 4259−4270.
(25) Wilson, C. C.; Morrison, C. A. *Chem. Phys. Lett.* **2002**, *362*, 85−89.
(26) Wilson, C. C. *New J. Chem.* **2002**, *26*, 1733−1739.
(27) Wilson, C. C. *Chem. Phys. Lett.* **2001**, *335*, 57−63.
(28) Wilson, C. C. *Acta Crystallogr., Sect. B: Struct. Sci.* **2001**, *B57*, 435−439.
(29) Wilson, C. C.; Shankland, K.; Shankland, N. *Z. Kristallogr.* **2001**, *216*, 303−306.
(30) Wilson, C. C.; Shankland, N.; Florence, A. J. *Chem. Phys. Lett.* **1996**, *253*, 103−107.
(31) Wilson, C. C.; Shankland, N.; Florence, A. J. *J. Chem. Soc., Faraday Trans.* **1996**, *92*, 5051−5057.
(32) Steiner, T.; Majerz, I.; Wilson, C. C. *Angew. Chem., Int. Ed.* **2001**, *40*, 2651−2654.
(33) Parkin, A.; Harte, S. M.; Goeta, A. E.; Wilson, C. C. *New J. Chem.* **2004**, *28*, 718−721.
(34) Bader, R. F. W. *Atoms Molecules: A Quantum Theory*; Oxford University Press: Oxford, UK, 1994.
(35) Bader, R. F. W. *NATO ASI Ser., Ser. B: Phys.* **1995**, *337*, 237−272.
(36) Bader, R. F. W. *NATO ASI Ser., Ser. C: Math. Phys. Sci.* **1993**, *406*, 313−349.
(37) Bader, R. F. W. *Chem. Rev. (Washington, D.C.)* **1991**, *91*, 893−928.
(38) Bader, R. F. W. *Acc. Chem. Res.* **1985**, *18*, 9−15.
(39) Nguyen-Dang, T. T.; Bader, R. F. W. *Physica A: Stat. Mech. Appl. (Amsterdam, Netherlands)* **1982**, *114A*, 68−73.
(40) Bader, R. F. W. http://www.chemistry.mcmaster.ca/faculty/bader/aim/.
(41) Dye, J. L. *Inorg. Chem.* **1997**, *36*, 3816−3826.
(42) Wagner, M. J.; Dye, J. L. *Annu. Rev. Mater. Sci.* **1993**, *23*, 223−253.
(43) Dye, J. L. *Science (Washington, D.C.)* **1990**, *247*, 663−668.
(44) Sheldrick, G. M. *SHELXL97, SHELXS97, SHELXTL*; University of Göttingen: Göttingen, Germany, 1997.
(45) Dickinson, R. G.; Raymond, A. L. *J. Am. Chem. Soc.* **1923**, *45*, 22−29.
(46) Gonell, H. W.; Mark, H. *Z. Phys. Chem.* **1923**, *107*, 181−218.
(47) Shaffer, P. A., Jr. *J. Am. Chem. Soc.* **1947**, *69*, 1557−1561.
(48) Andresen, A. F. *Acta Crystallogr.* **1957**, *10*, 107−110.
(49) Becka, L. N.; Cruickshank, D. W. J. *Proc. R. Soc. (London)* **1963**, *273*, 455−465.
(50) Becka, L. N.; Cruickshank, D. W. J. *Proc. R. Soc. (London)* **1963**, *273*, 435−454.
(51) Duckworth, J. A. K.; Willis, B. T. M.; Pawley, G. S. *Acta Crystallogr., Sect. A: Cryst. Phys., Diffr., Theor. Gen. Crystallogr.* **1969**, *25*, 482−484.
(52) Willis, B. T. M.; Howard, J. A. K. *Acta Crystallogr., Sect. A: Cryst. Phys., Diffr., Theor. Gen. Crystallogr.* **1975**, *A31*, 514−520.
(53) Parini, E. V.; Tsirel'son, V. G.; Ozerov, R. P. *Kristallografiya* **1985**, *30*, 857−866.
(54) Chekhlov, A. N.; Ionov, S. P. *Kristallografiya* **1982**, *27*, 506−510.
(55) Grochowski, J.; Serda, P.; Wilson, K. S.; Dauter, Z. *J. Appl. Crystallogr.* **1994**, *27*, 722−726.

(56) Kampermann, S. P.; Sabine, T. M.; Craven, B. M.; McMullan, R. K. *Acta Crystallogr., Sect. A: Found. Crystallogr.* **1995**, *A51*, 489−497.
(57) Spackman, M. A.; Byrom, P. G. *Acta Crystallogr., Sect. B: Struct. Sci.* **1997**, *B53*, 553−564.
(58) Terpstra, M.; Craven, B. M.; Stewart, R. F. *Acta Crystallogr., Sect. A: Found. Crystallogr.* **1993**, *A49*, 685−692.
(59) Resing, H. A. *Mol. Cryst. Liq. Cryst.* **1969**, *9*, 101−132.
(60) Burgi, H. B.; Capelli, S. C.; Birkedal, H. *Acta Crystallogr., Sect. A: Found. Crystallogr.* **2000**, *A56*, 425−435.
(61) Mak, T. C. W.; Ladd, M. F. C.; Povey, D. C. *J. Chem. Soc., Perkin Trans. 2: Phys. Org. Chem.* **1979**, 593−595.
(62) Bruno, I. J.; Cole, J. C.; Edgington, P. R.; Kessler, M.; Macrae, C. F.; McCabe, P.; Pearson, J.; Taylor, R. *Acta Crystallogr., Sect. B* **2002**, *B58*, 389−397.
(63) Allen, F. H.; Motherwell, W. D. S. *Acta Crystallogr., Sect. B* **2002**, *B58*, 407−422.
(64) Yu, P.-Y.; Mak, T. C. W. *Acta Crystallogr., Sect. B: Struct. Crystallogr. Cryst. Chem.* **1978**, *B34*, 3053−3056.
(65) Trotter, J.; Mak, T. C. W. *Acta Crystallogr., Sect. B: Struct. Crystallogr. Cryst. Chem.* **1979**, *B35*, 2367−2369.
(66) Mak, T. C. W.; Lam, Y.-S. *Acta Crystallogr., Sect. B: Struct. Crystallogr. Cryst. Chem.* **1978**, *B34*, 1732−1735.
(67) Lam, Y.-S.; Mak, T. C. W. *Acta Crystallogr., Sect. B: Struct. Crystallogr. Cryst. Chem.* **1978**, *B34*, 1915−1918.
(68) Lam, Y.-S.; Mak, T. C. W. *Aust. J. Chem.* **1978**, *31*, 1249−1253.
(69) Chesnut, D. B.; Savin, A. *J. Am. Chem. Soc.* **1999**, *121*, 2335−2336.
(70) Chesnut, D. B. *J. Am. Chem. Soc.* **1998**, *120*, 10504−10510.
(71) Cunningham, T. P.; Cooper, D. L.; Gerratt, J.; Karadakov, P. B.; Raimondi, M. *J. Chem. Soc., Faraday Trans.* **1997**, *93*, 2247−2254.
(72) Cunningham, T. P.; Cooper, D. L.; Gerratt, J.; Karadakov, P. B.; Raimondi, M. *Int. J. Quantum Chem.* **1996**, *60*, 393−400.
(73) Rai, U. S.; Symons, M. C. R. *J. Chem. Soc., Faraday Trans.* **1994**, *90*, 2649−2652.
(74) Gilheany, D. G. *Chem. Rev.* **1994**, *94*, 1339−1374.
(75) Magnusson, E. *J. Am. Chem. Soc.* **1993**, *115*, 1051−1061.
(76) Reed, A. E.; Schleyer, P. v. R. *J. Am. Chem. Soc.* **1990**, *112*, 1434−1445.
(77) *Smart*, Version 5.044; Bruker: Madison, WI, 1997.
(78) *Saint*, Version 5.01; Bruker: Madison, WI, 1997.
(79) Larson, A. C.; Von Dreele, R. B. *General Structure Analysis System (GSAS)*; Los Alamos National Laboratory: Los Alamos, NM, 2000.
(80) Sheldrick, G. M. *SADABS*; University of Göttingen: Göttingen, Germany, 1996.
(81) Schultz, A. J.; Srinivasan, K.; Teller, R. G.; Williams, J. M.; Lukehart, C. M. *J. Am. Chem. Soc.* **1984**, *106*, 999−1003.
(82) Schultz, A. J.; Carlin, R. L. *Acta Crystallogr., Sect. B: Struct. Sci.* **1995**, *B51*, 43−47.
(83) Chatterjee, A.; Mikkelson, D.; Mikkelson, R.; Hammonds, J.; Worlton, T. *Appl. Phys. A: Mater. Sci. Process.* **2002**, *74*, S194−S197.
(84) Sears, V. F. *Methods of Experimental Physics*; Academic Press: New York, 1986; Vol. 23.
(85) Howard, J. A. K.; Johnson, O.; Schultz, A. J.; Stringer, A. M. *J. Appl. Crystallogr.* **1987**, *20*, 120−122.
(86) Taylor, R.; Macrae, C. F. *Acta Crystallogr., Sect. B* **2001**, *B57*, 815−817.
(87) Desiraju, G. R.; Steiner, T. *The Weak Hydrogen Bond*; Oxford University Press: New York, 2001; Vol. 9.
(88) Bondi, A. *J. Phys. Chem.* **1964**, *68*, 441−451.
(89) Steiner, T.; Desiraju, G. R. *Chem. Commun.* **1998**, 891−892.
(90) Wilson, C. C.; Goeta, A. E. *Angew. Chem., Int. Ed.* **2004**, *43*, 2095−2099.
(91) Nygren, C. L.; Wilson, C. C.; Turner, J. F. C. Accepted for publication in *J. Phys. Chem. A.*
(92) Dunitz, J. D.; Schomaker, V.; Trueblood, K. N. *J. Phys. Chem.* **1988**, *92*, 856−867.
(93) Fenn, T. D.; Ringe, D.; Petsko, G. A. *J. Appl. Crystallogr.* **2003**, *36*, 944−947.
(94) Farrugia, L. J. *J. Appl. Crystallogr.* **1999**, *32*, 837−838.